Published in final edited form as:
*Chem Sci*. 2013 July 1; 4(7): . doi:10.1039/C3SC50462J.

# Halogen Photoelimination from Dirhodium Phosphazane Complexes via Chloride-Bridged Intermediates

**David C. Powers**[a,b], **Matthew B. Chambers**[a,b], **Thomas S. Teets**[a], **Noémie Elgrishi**[a], **Bryce, L. Anderson**[a,b], and **Daniel G. Nocera**[a,b]

[a] Department of Chemistry, 6-335, Massachusetts Institute of Technology, 77 Massachusetts Avenue, Cambridge, Massachusetts 02139-4307, U.S.A.

[b] Department of Chemistry and Chemical Biology, 12 Oxford Street, Cambridge, MA 02138–2902.

## Abstract

Halogen photoelimination is a critical step in HX-splitting photocatalysis. Herein, we report the photoreduction of a pair of valence-isomeric dirhodium phosphazane complexes, and suggest that a common intermediate is accessed in the photochemistry of both mixed-valent and valence-symmetric complexes. The results of these investigations suggest that halogen photoelimination proceeds by two sequential photochemical reactions: ligand dissociation followed by subsequent halogen elimination.

## Introduction

Photochemical HX splitting reactions (X = halogen) provide an avenue towards solar-to-fuels energy conversion schemes.[1] We have targeted two-electron, mixed-valent dirhodium phosphazane complexes as catalyst platforms for photochemical HX splitting reactions[2–5] based on the precept that: (i) the M–M bond, which is conserved across the $d^9$–$d^9$, $d^7$–$d^9$, $d^7$–$d^7$ series, could act as a chromophore to drive both $H_2$- and $X_2$-forming reactions;[6] and, (ii) ground-state two-electron mixed valency may afford excited states that participate in two-electron photoredox chemistry in preference to undesired one-electron reactions.[7,8] Halogen reductive elimination is a challenging transformation.[9-11] While halide oxidation is



Correspondence to: Daniel G. Nocera.

dnocera@fas.harvard.edu..

†Electronic Supplementary Information (ESI) available: Experimental procedures and time-dependent photochemical data; detailed computational methods and XYZ coordinates for all computed structures. See DOI: 10.1039/b000000x/

‡Crystallographic data for **1**: $C_{40}H_{52}Cl_4F_{24}N_3O_8P_4Rh_2$, $M$ = 1644.35, Monoclinic, $P2_1/n$, $a$ = 12.7242 (5), $b$ = 20.3878(8), $c$ = 23.2389(9), β = 97.497(1)°, V = 5977.1(4), Z = 4, μ = 0.95 $mm^{-1}$, T = 100(2) K, $R_1$ = 0.0747, $wR_2$ = 0.1231 (based on all reflections), GooF = 1.012, reflections measured = 17477, unique reflections = 12674, $R_{int}$ = 0.063. Crystallographic data for **6**: $C_{25}H_{26}Cl_2F_{25}N_3O_8P_4Rh_2$, $M$ = 1372.09, Triclinic, $P1$, $a$ = 10.1595(9), $b$ = 10.386(1), $c$ = 12.0283(11), α = 73.963(2)° β = 69.049(1)°, γ = 71.477(2)°, V = 1104.74(18), Z = 1, μ = 1.17 $mm^{-1}$, T = 100(2) K, $R_1$ = 0.0439, $wR_2$ = 0.0849 (based on all reflections), GooF = 1.033, reflections measured = 12490, unique reflections = 11183, $R_{int}$ = 0.036. Crystallographic data for **7**: $C_{26}H_{29}Cl_2F_{24}N_3O_9P_4Rh_2$, $M$ = 1384.12, Monoclinic, $P2_1/c$, $a$ = 12.0403(8), $b$ = 19.3984(13), $c$ = 20.6248(14), β = 106.961(1)°, V = 4607.6(5), Z = 4, μ = 1.12 $mm^{-1}$, T = 100(2) K, $R_1$ = 0.0674, $wR_2$ = 0.1006 (based on all reflections), GooF = 1.029, reflections measured = 8770, unique reflections = 6365, $R_{int}$ = 0.036. Crystallographic data for **8**: $C_{25}H_{26}Cl_4F_{25}N_3O_8P_4Rh_2$, $M$ = 1442.99, Monoclinic, $P2_1/c$, $a$ = 12.2025(13), $b$ = 21.385(2), $c$ = 20.398(2), β = 98.351(2)°, V = 5266.4(10), Z = 4, μ = 1.08 $mm^{-1}$, T = 100(2) K, $R_1$ = 0.0915, $wR_2$ = 0.2042 (based on all reflections), GooF = 1.054, reflections measured = 10776, unique reflections = 8406, $R_{int}$ = 0.000. Crystallographic data for **9**: $C_{33}H_{37}Cl_4F_{24}N_3O_9P_4Rh_2$, $M$ = 1547.16, Triclinic, $P1$, $a$ = 10.7825(5), $b$ = 15.2029(8), $c$ = 18.7253(9), α = 87.983(1)°, β = 80.065(1)°, γ = 73.223(1)°, V = 2894.5(2), Z = 2, μ = 0.99 $mm^{-1}$, T = 100(2) K, $R_1$ = 0.0656, $wR_2$ = 0.1598 (based on all reflections), GooF = 1.053, reflections measured = 14427, unique reflections = 12029, $R_{int}$ = 0.038.

typically the turnover-limiting step in HX-splitting photocatalysis.[12–14] the mechanism of photoreduction remains largely unknown.[15]

Herein, we report the photoreduction of two dirhodium valence isomers: a two-electron, mixed-valence $Rh_2$[I,III] complex **1** and a valence-symmetric $Rh_2$[II,II] complex **2**. Transient spectroscopy experiments suggest that two complexes proceed through a common photochemical intermediate, which we propose to be a chloride-bridged structure based on the independent preparation of chloride-bridged complexes that are faithful models of the intermediate. Direct interrogation of the reactivity of these chloride-bridged complexes has led to the proposal that halogen elimination proceeds by sequential ligand photodissociation to afford the chloride-bridged intermediate followed by halogen photoelimination.

## Experimental

Complexes **2** and **3** were prepared according to previously reported procedures.[4] Compounds **6** and **7** were delivered by sequential treatment of a THF solution of $[Rh(cod)Cl]_2$ with tfepma (tfepma = *bis*(trifluoroethoxy)phosphinyl)methylamine) and then *p*-fluorophenylisocyanide or *p*-methoxyphenyl-isocyanide, respectively. The reaction solution was stirred at room temperature, and upon completion of the reaction, the solvent was removed in vacuo. The residue was taken up in THF and hexanes, the supernatant was removed, and the solid residue was dried in vacuo to afford the orange solids of **6** and **7** in 59% and 65% yields, respectively. Complexes **1**, **8** and **9** were furnished by treatment of saturated toluene solution s of the parent complexes, **3**, **6** and **7**, respectively, with excess of $PhICl_2$. The reaction proceeded over hours at room temperature or with modest heating. The product was obtained typically by removing solvent in vacuo and taking up the residue in toluene and then cooling. The green solid of **1** was obtained in 88% yield, a dark orange solid of **8** was obtained in 94% yield and the red-orange solid of **9** was obtained in 88% yield. Crystals of **1**, **6**, **7**, **8** and **9** that were suitable for X-ray diffraction analysis were grown from toluene.

Compounds **1** and **2** were photolyzed with the broadband excitation light delivered from a 1000 W Hg/Xe arc lamp equipped with long-pass filters, respectively. THF solutions of the complexes were photolyzed in 1 cm quartz cuvettes. Reaction samples were periodically removed from the light source and UV-vis spectra were recorded. Photolysis spectra are shown in Figs. S15 and S16 for $\lambda_{exc} > 295$ nm for **1** and **2**, respectively, and in Fig. S17 for **1** with $\lambda_{exc} > 380$ nm. The concentrations of photoreactants and photoproducts during the course of the irradiation were determined from least-squares fitting of the time-evolved spectra.

## Results and Discussion

While developing the new structural class of HCl-splitting dirhodium photocatalysts that is summarized in Scheme 1,[4] we isolated two dirhodium valence isomers: two-electron mixed-valent $Rh_2$[I,III] complex **1** and valence-symmetric $Rh_2$[II,II] complex **2**. Complex **1** is accessed by oxidation of $Rh_2$[0,II] complex **3** with $PhICl_2$ whereas complex **2** is prepared by aerobic oxidation of **3** in the presence of HCl. **1** and **2** undergo photoreduction under identical conditions (Fig. 1).

Photolysis of a THF solution of **1**, which displays absorbance features at 329 and 379 nm, with a 1000 W Hg/Xe lamp ($\lambda > 295$nm) resulted in the consumption of **1** and eventual formation of $Rh_2$[0,II] complex **3**. The absence of isosbestic points in the photolysis spectrum (Fig. 2a) indicated the photoevolution of a steady-state intermediate. $^{31}$P NMR

analysis of an experiment in which complex **1** was photolyzed in an NMR tube established the steady-state intermediate to be valence-symmetric complex **2** (Fig. S18).

Complex **1** displays wavelength-selective photochemistry. Photolysis of **1** with a 380 nm long-pass filter, used to selectively excite the lower-energy absorption band of **1** ($\lambda_{max}$ =379 nm), resulted in the exclusive isomerization of **1** to **2** (Fig. S17). These results establish that photoreduction of **1** to **3** is driven by excitation into the 329-nm absorbance band whereas isomerization of **1** to **2** arises from excitation into the 379-nm absorption band. Independent photolysis of a THF solution of **2**, which displays an absorbance feature at 352 nm, afforded $Rh_2$[0,II] complex **3**. Well-anchored isosbestic points are observed in the UV-vis photolysis spectrum of **2** (Fig. 3a), excluding the evolution of a steady-state intermediate in the photolysis of **2**.

With knowledge of the molar absorptivities of complexes **1**, **2** and **3**, the concentration of each of these species during photolysis was determined using least-squares spectral fitting of the UV-vis spectra. As shown in Fig. 2b, the concentration of $Rh_2$[II,II] complex **2** initially builds and subsequently decays during the photolysis of $Rh_2$[I,III] complex **1**. Similar analysis was carried out on the photolysis of $Rh_2$[II,II] complex **2** and confirmed that no appreciable concentration of Rh[I,III] complex **1** evolves with time (Fig. 3b). The observed photoreduction chemistry of both mixed-valent complex **1** and valence-symmetric complex **2** provided the first opportunity to experimentally probe the importance of mixed valency in halogen elimination from dirhodium complexes.

In order to assess the relative efficiencies of halogen elimination from $Rh_2$[I,III] complex **1** and $Rh_2$[II,II] complex **2**, we determined the quantum yields for photoelimination from each of these complexes. Direct comparison of halogen elimination efficiencies was complicated by competing elimination and isomerization reactions in the photochemical manifold of **1**. At early times during the photolysis of $Rh_2$[I,III] complex **1**, the observed quantum yield for the consumption of **1** ($\Phi_{320}$ = 0.36%), represents both photoreduction of **1** to **3**, as well of photoisomerization of **1** to **2**. The quantum yield of photoisomerization was determined by evaluating the consumption of **1** during the period of photolysis in which the concentration of **2** is approximately constant (after approximately 20% of **1** has been consumed). In this pseudo-state-state regime, the quantum efficiency of photoisomerization was determined to be 0.07%. By difference, the quantum efficiency of photoreduction of **1** was determined to be 0.29% and the quantum efficiency of halogen photoelimination from $Rh_2$[II,II] complex **2** was determined to be 0.47%. Thus photoreduction of **2** is slightly more efficient than of **1**.

Based on the similarity of the quantum yields for photoreduction of complexes **1** and **2**, respectively, we posited that a common intermediate may be accessed in the photochemical manifold of these complexes. To evaluate this contention, flash laser photolysis ($\lambda_{exc}$ = 355 nm) of complexes **1** and **2** was carried out and the transient absorption (TA) difference spectra shown in Fig. 4 were obtained. The TA spectrum of **1** exhibits ground-state bleaches at 329 and 379 nm and a spectral growth at ~440 nm. The new spectral feature at ~440 nm is not an absorption feature of either **2** or **3** and thus represents a species that is not observed in the steady-state photolysis experiment. Flash laser photolysis of complex **2** revealed a TA spectrum with a ground-state bleach at ~350 nm and also a spectral growth at ~440 nm. Excepting a narrower line-shape for the absorbance feature of **1**, the transient absorption spectra of **1** and **2** are very similar for $\lambda_{exc}$ > 400 nm. This narrowing of the 440 nm TA signal of **1** is consistent with a superposition of a ground state bleach centered at ~460 nm with the spectral growth at ~440 nm. Owing to the similarities of the transient profiles of **1** and **2** at $\lambda$ > 400 nm, we propose that photolysis of **1** and **2** affords a common intermediate.

To gain insight into the nature of the excited states of **1** and **2** that lead to the observed photochemical intermediates, time-dependent DFT (TD-DFT) calculations were performed with Gaussian 03[16] and the B3LYP functionals[17,18] using model complexes $Rh^{I,III}(dfpma)_2(CNMe)_2Cl_4$ (**A**) and $Rh^{II,II}(dfpma)_2$-$(CNMe)_2Cl_4$ (**B**) (Fig. 5). In model structures, **A** and **B**, the adamantyl isocyanide ligand was replaced with a methyl isocyanide and the bridging tfepma ligands were replaced with *bis*(diflurophosphinyl)methylamine (dfpma) ligands. Similar structural truncations have been validated in TD-DFT calculations of several heterobimetallic complexes.[15,19,20] The optimized geometries and computed absorption spectra of **A** and **B** reproduced both the metrical parameters and experimental absorption spectra of **1** and **2**, respectively.

The computed excited states of both structures **A** and **B** are dominated by ligand-to-metal charge transfer (LMCT) character; the excited states computed for both **A** and **B** have M–M σ* and M–P σ* character (Fig. 5). We have considered the strongest oscillator strength in the spectral absorbance envelop near 320 nm; evaluation of the orbital parentage of the major absorbance revealed that in both complexes, the LMCT excitations are primarily Cl (p) → Rh (d) + dfpma (p) transitions. For $Rh_2$(I,III) structure **A**, the transition is calculated to occur from a ground state orbital that is 30% Rh, 60% Cl, and 7% dfpma to an excited state orbital that is 40% Rh, 8% Cl, 36% dfpma. Similarly, $Rh_2$(II,II) complex **B**, excitation results in a transition from a ground state orbital that is 20% Rh, 73% Cl, and 2% dfpma, to an excited state orbital that is 42% Rh, 15% Cl, and 30% dfpma. In contrast, analysis of the absorbance feature of **1** near $\lambda_{max}$ = 379 nm, which results in isomerization of **1** to **2** when excited, features transitions that reduce both the Rh(III) center and the Cl ligands.

In analogy to the hydride-bridged transition states, which have been proposed for $H_2$ evolving reactions from diiridium complexes,[7,8] we propose that the photointermediate in the TA spectrum is chloride-bridged structure **5** (Fig. 6). Accessing intermediate **5** from either mixed-valent complex **1** or valence-symmetric complex **2** could be accomplished by photochemically promoted dissociation of an isocyanide ligand. This ligand dissociation could proceed heterolytically, as shown in Fig. 6, or homolytically, to generate unsaturated intermediates reduced by one electron as compared with **1**. The TD-DFT calculations support this proposal. The computed excited states of both **A** and **B** are dissociative with respect to the Rh–isocyanide bond, which is consistent with loss of an isocyanide to generate the coordination site needed for a chloride-bridged structure. Isomerization of **1** to **2** may be accomplished by a similar mechanism, in which dissociation of chloride, not isocyanide, would generate an open coordination site to accommodate a bridging isocyanide (i.e. intermediate **4**). Re-coordination of chloride to the formerly Rh(III) center would affect net isomerization. Such a proposal is supported by the observation that the lower energy excitation of **1**, which is dissociative with respect to the Rh(III)–Cl bonds and thus could generate a vacant coordination site for a bridging isocyanide ligand, promotes isomerization of **1** to **2** (i.e. structure **4**).

In the mechanism outlined in Fig. 6, dirhodium complexes with bridging chloride and isocyanide ligands are the intermediates in chlorine elimination and isomerization, respectively. With interest in establishing that the proposed bridging-ligand geometries are accessible in phosphazane-supported dirhodium architectures, as well as directly interrogating the photochemistry of chloride-bridged dirhodium complexes, a new family of ligand-bridged dirhodium complexes was prepared (Fig. 7). Treatment of $[Rh(cod)Cl]_2$ in THF with tfepma and either 4-fluorophenyl or 4-methoxyphenyl isocyanide resulted in the formation of isocyanide bridged complexes **6** and **7**, respectively. Complexes **6** and **7** do not react with excess isocyanide. Oxidation of $Rh_2$[I,I] complexes **6** and **7** with $PhICl_2$ afforded chloride-bridged structures **8** and **9**, respectively. Analysis of the IR spectra of **6** and **8** confirmed that the isocyanide ligand migrates from a bridging to terminal binding

coordination position upon oxidation; the isocyanide stretching frequency in **6** (1736 $cm^{-1}$) moves to higher energy in **8** (2181 $cm^{-1}$). The structures of complexes **6–9** have all been established by single-crystal x-ray diffraction. Importantly, access to isolable models of proposed intermediate **5** allowed comparison of the absorption spectra of the model complexes with the absorption features observed in the TA spectra. In the absorption spectra of both **8** and **9**, an absorption feature centered at ~450 nm is observed (Fig. S34), which is consistent with our assignment of intermediate **5** in the TA spectra as well as a TD-DFT calculation of a truncated model of **5** (Figs. S44 and S45).

With chloride-bridged dirhodium complexes in hand, the photoreactivity of these species was investigated. Photolysis of a THF solution of chloride-bridged complex **8** effected photoreduction, yielding $Rh_2$[I,I] complex **6** ($\Phi_{320}$ = 0.80; Fig. 8). During the observed photoreduction, the isocyanide ligand moved from a ter minal binding mode to a bridging geometry, which may be responsible for the ability to observe photoreduction products in the absence of exogenous stabilizing ligands. We note that no reduction was observed upon thermolysis of complex **8** at 80 °C in the dark. The observation of a photochemically, but not thermally, promoted reduction of **8** suggests that photoreduction of complexes **1** and **2** proceeds by two sequential photochemical reactions, the first of which generates chloride-bridged intermediate **5** from which photoelimination proceeds.

## Conclusions

Formal chlorine photoelimination occurs from both mixed-valent $Rh_2$[I,III] complex **1** and valence-symmetric $Rh_2$[II,II] complex **2** with similar efficiencies. Transient absorption studies suggest that the photochemistry of **1** and **2** proceed through a common intermediate, which propose to be chloride-bridged structure **5**. The presence of a common intermediate (i.e. **5**) in the photochemical manifold of both complex **1** as well as **2** implies that the observed differences in photoreduction ef ficiency between complexes **1** and **2** is due to the differing efficiencies associated with accessing **5**, and not to the halogen elimination reaction itself. The observation of photochemically, but not thermally, promoted reduction of isolated models of intermediate **5** (i.e. chloride-bridged complex **8**) suggests that overall photoreduction of **1** and **2** proceeds by two sequential photochemical steps: ligand dissociation followed by halogen elimination. New HX-splitting photocatalysts, in which photochemically promoted ligand dissociation is not prerequisite for halogen elimination, may be more efficient because photoreduction would require one, not two, photochemical events. We therefore postulate that the highest photoelimination quantum efficiencies will be achieved for complexes that can directly assume a halide-bridged structure.

## Supplementary Material

Refer to Web version on PubMed Central for supplementary material.

## Acknowledgments

We gratefully acknowledge funding from NSF Grant CHE-1112154. D.C.P. is supported by a Ruth L. Kirchenstein National Research Service award (F32GM103211) and T.S.T acknowl edges the Fannie and John Hertz Foundation for a graduate research fellowship.

## references

1. Esswein AJ, Nocera DG. Chem. Rev. 2007; 107:4022. [PubMed: 17927155]
2. Heyduk AF, Nocera DG. Science. 2001; 293:1639. [PubMed: 11533485]
3. Esswien AJ, Veige AS, Nocera DG. J. Am. Chem. Soc. 2005; 127:16641. [PubMed: 16305253]

4. Elgrishi N, Teets TS, Chambers MB, Nocera DG. Chem. Commun. 2012; 48:9474.
5. Recently, halogen photoelimination from a PtTe heterobimetallic has been disclosed: Lin T-P, Gabbaï FP. J. Am. Chem. Soc. 2012; 134:12230. [PubMed: 22708610]
6. Heyduk AF, Nocera DG. Chem. Commun. 1999:1519.
7. Gray TG, Veige AS, Nocera DG. J. Am. Chem. Soc. 2004; 126:9760. [PubMed: 15291579]
8. Nocera DG. Inorg. Chem. 2009; 48:10001. [PubMed: 19775081]
9. Van Zyl WE, López-de-Luzuriaga JM, Fackler JP Jr. Staples RJ. Can. J. Chem. 2001; 79:896.
10. Fackler JP Jr. Inorg. Chem. 2002; 41:6959. [PubMed: 12495334]
11. Ovens JS, Leznoff DB. Dalton. Trans. 2011; 40:4140. [PubMed: 21394363]
12. Cook TR, Esswein AJ, Nocera DG. J. Am. Chem. Soc. 2007; 129:10094. [PubMed: 17655239]
13. Cook TR, Surendranath Y, Nocera DG. J. Am. Chem. Soc. 2009; 131:28. [PubMed: 19093813]
14. Teets TS, Nocera DG. J. Am. Chem. Soc. 2009; 131:7411. [PubMed: 19422239]
15. Cook TR, McCarthy BD, Lutterman DA, Nocera DG. Inorg. Chem. 2012; 51:5152. [PubMed: 22475040]
16. Frisch, MJ., et al. *Gaussian 03*, revision B.05. Gaussian, Inc.; Wallingford, CT: 2004.
17. Lee C, Yang W, Parr RG. Phys. Rev. B. 1988; 37:785.
18. Miehlich B, Savin A, Stoll H, Preuss H. Chem. Phys. Lett. 1989; 157:200.
19. Teets TS, Lutterman DA, Nocera DG. Inorg. Chem. 2010; 49:3035. [PubMed: 20166685]
20. Esswein AJ, Dempsey JL, Nocera DG. Inorg. Chem. 2007; 46:2362. [PubMed: 17326627]

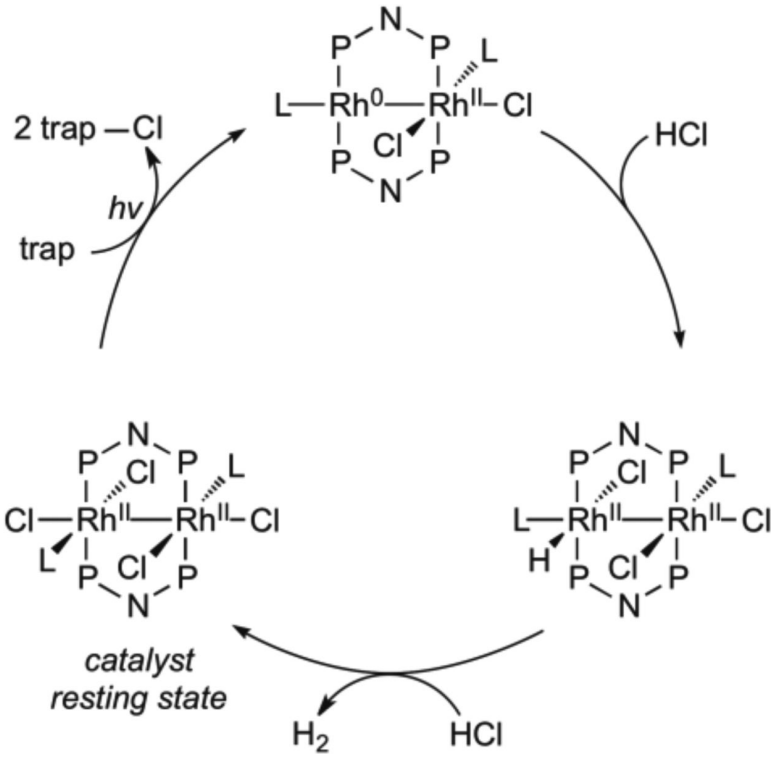


**Scheme 1.**
Catalysis cycle for photocatalytic HCl splitting.

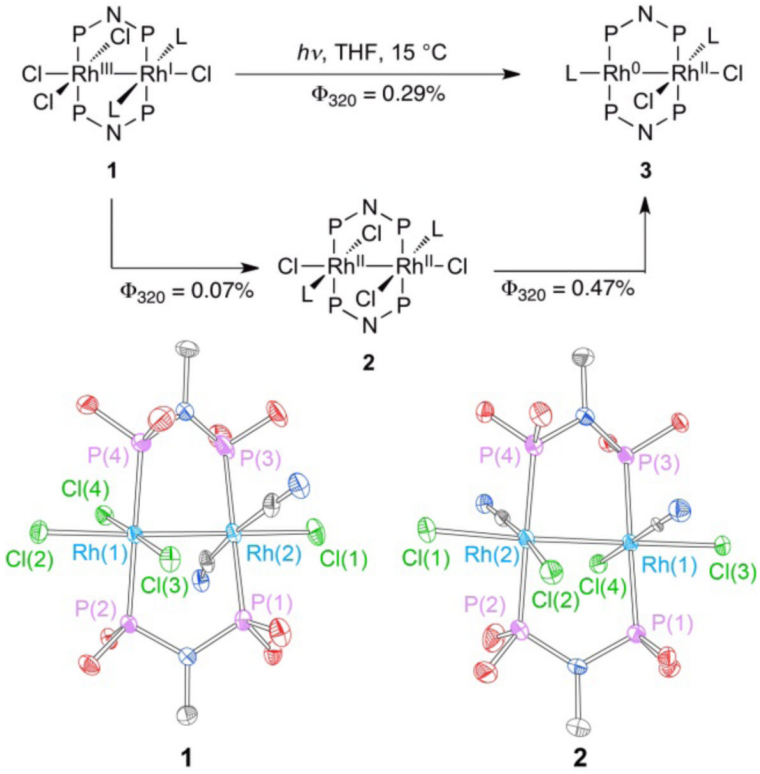


**Fig. 1.**

Photolysis of two-electron mixed-valent $Rh_2$[I,III] complex **1** affords $Rh_2$[0,II] complex **3** via both direct halogen elimination, as well as isomerization to valence-symmetric $Rh_2$[II,II] **2**, which undergoes halogen elimination; L = 1-adamantylisocyanide, P–N–P = *bis*(trifluoroethoxy)phosphinyl)methylamine (tfepma). Thermal ellipsoid plots of **1** and **2** drawn at the 50% probability level. The $–CH_2CF_3$, adamantly groups and hydrogen atoms are omitted for clarity.

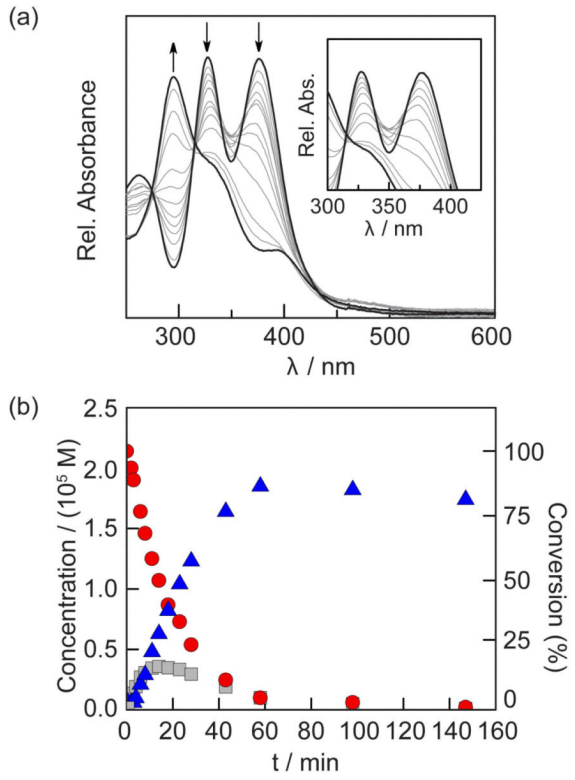


**Fig. 2.**

(a) Spectral evolution during photolysis of $Rh_2$[I,III] complex **1** in THF. Inset: Expanded spectrum to show that isosbestic points are not observed, consistent with evolution of a steady-state intermediate during the photolysis of **1**. (b) Concentration profiles of **1** (red circle), **2** (gray square) and **3** (blue triangle) during the photolysis of **1**.

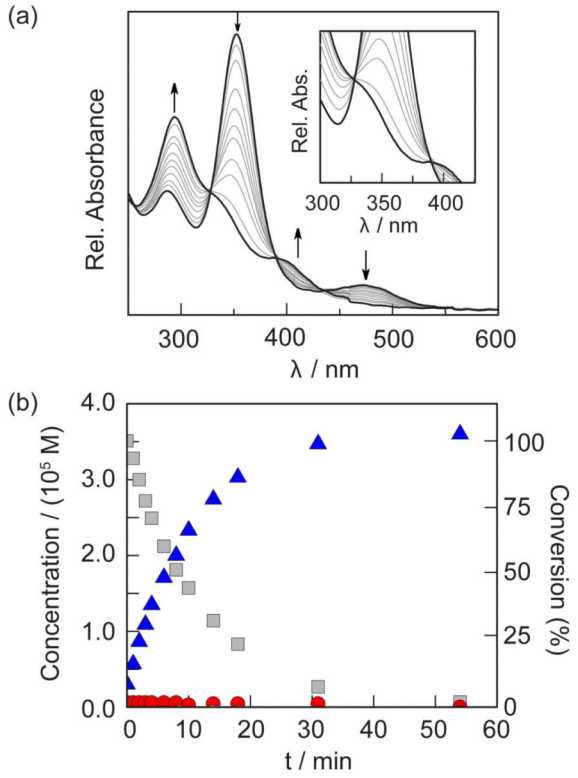


**Fig. 3.**

(a) Spectral evolution during photolysis of $Rh_2$[II,II] complex **2** in THF. Inset: Expanded spectrum to show that isosbestic points are observed, precluding a steady-state intermediate. (b) Concentration profiles of **1** (red circle), **2** (gray square) and **3** (blue triangle) during the photolysis of **2**.

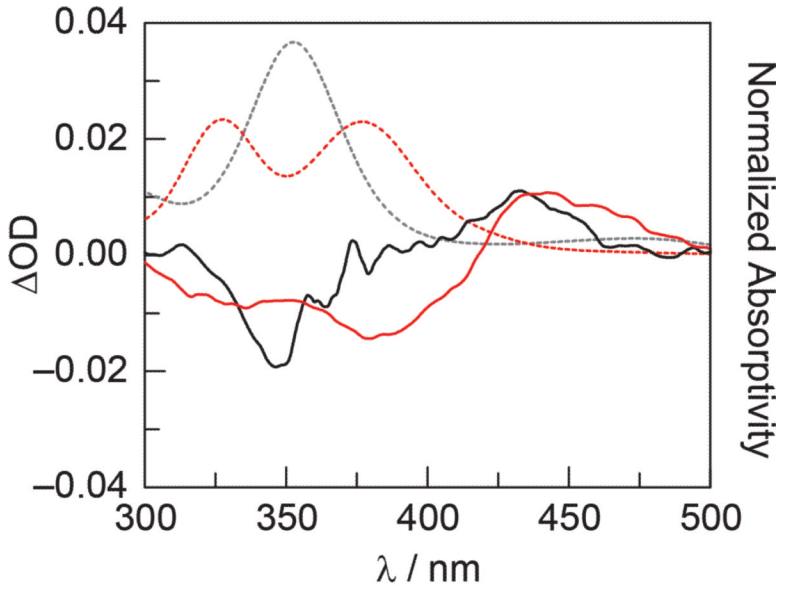


**Fig. 4.**

Transient absorption spectra obtained by laser flash photolysis ($\lambda_{exc}$ = 355 nm) of complexes **1** (solid red) and **2** (solid black), respectively. Spectra are normalized to the absorbance at ~440 nm. Normalized absorption spectra of **1** (dashed red) and **2** (dashed black) are also shown

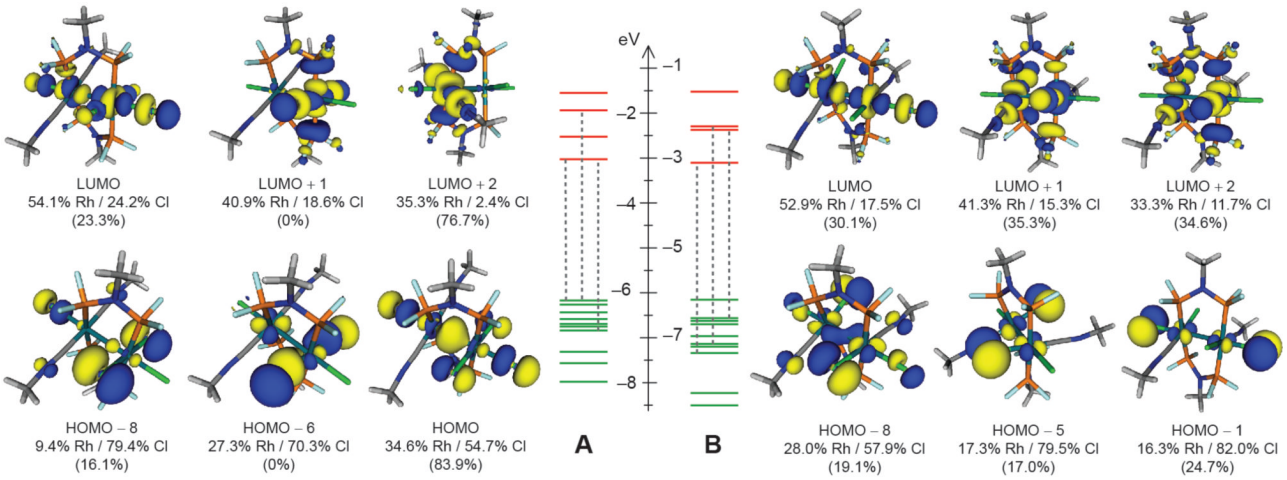


**Fig. 5.**

TD-DFT calculations of model structures **A** and **B** indicate LMCT excited state in both complexes. Contributions of Rh-based and Cl-based orbitals are given for each individual MO. Contributions of each MO to the overall electronic transformation are given within parentheses.

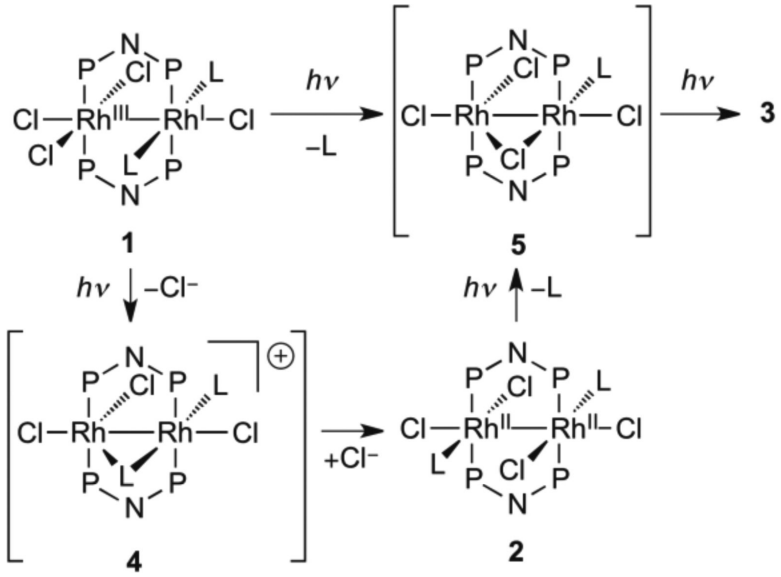


**Fig. 6.**
Proposed mechanisms for isomerization and photoreduction reactions.

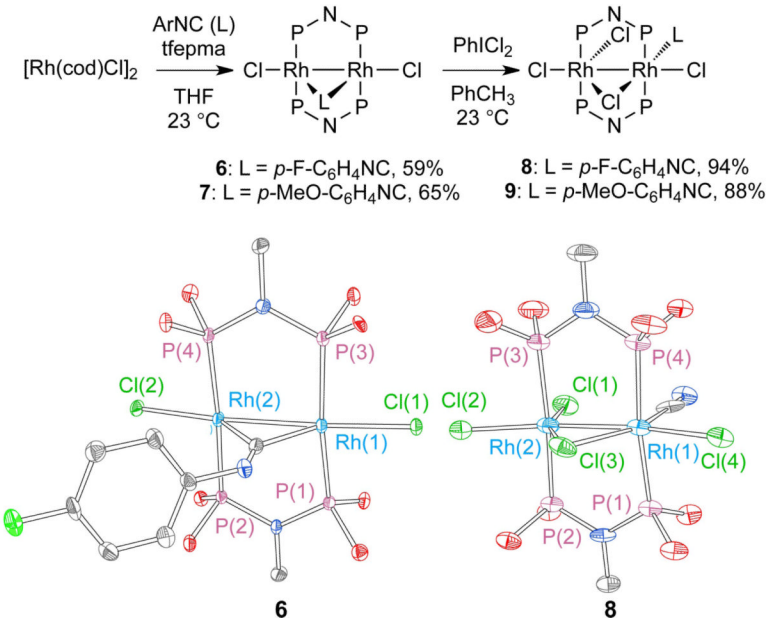


**Fig. 7.**

Synthesis of isocyanide-bridged (**6** and **7**) and chloride-bridged (**8** and **9**) dirhodium complexes, P–N–P = *bis*(trifluoroethoxy)phosphinyl)-methylamine (tfepma). Thermal ellipsoid plots of **6** and **8** drawn at the 50% probability level. The $–CH_2CF_3$, hydrogen atoms, and the 4-fluorophenyl group from **8** are omitted for clarity.

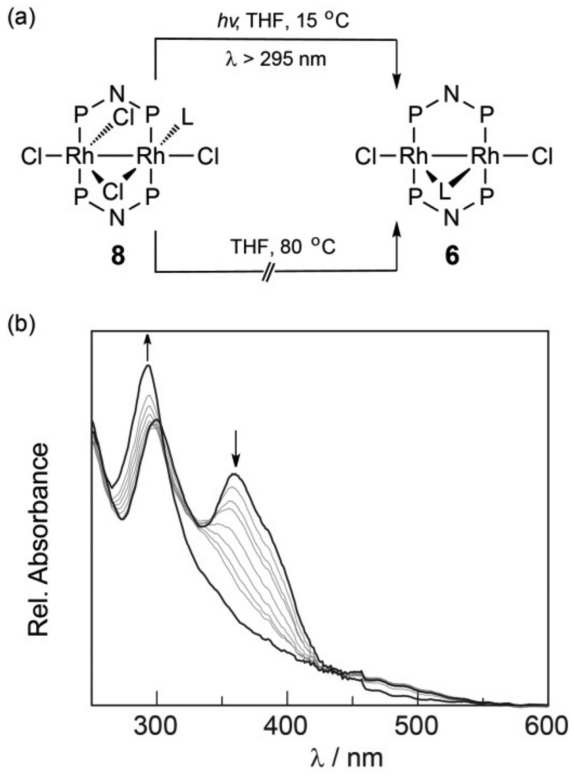


**Fig. 8.**

(a) Chloride-bridged dirhodium complex **8** undergoes photochemical, but not thermal, chlorine elimination to afford $Rh_2$[I,I] complex **6**. (b) Spectral evolution during photolysis of chloride-bridged complex **8**.